ARTICLES
https://doi.org/10.1038/s41929-017-0005-1
nature catalysis

Technical photosynthesis involving CO_2 electrolysis and fermentation

Thomas Haas[1], Ralf Krause[2], Rainer Weber[3], Martin Demler[1] and Guenter Schmid[2]*

Solar-powered electrochemical reduction of CO_2 and H_2O to syngas, followed by fermentation, could lead to sustainable production of useful chemicals. However, due to insufficient electric current densities and instabilities of current CO_2-to-CO electrolysers, a practical, scalable artificial photosynthesis remains a major challenge. Here, we address these problems using a commercially available silver-based gas diffusion electrode (used in industrial-scale chlorine–alkaline electrolysis) as the cathode in the CO_2 electrolyser. Electric current densities up to 300 mA cm^{-2} were demonstrated for more than 1,200 hours with continuous operation. This CO_2 electrolyser was coupled to a fermentation module, where the out-coming syngas from the CO_2 electrolyser was converted to butanol and hexanol with high carbon selectivity. Conversion of photovoltaic electricity, CO_2 and H_2O to the desired alcohols achieved close to 100% Faradaic efficiency. Industrial production of useful and high-value chemicals via artificial photosynthesis is closer than expected with the proposed scalable hybrid system.

High-value organic chemicals, such as butanol and hexanol, have multiple applications in coatings, chemical synthesis, and as solvents and fuels. Currently, about four million metric tonnes of 1-butanol are produced worldwide. In Germany, about 0.6 million metric tonnes of 1-butanol are produced from fossil fuels per year[1]. Until now, these organic chemicals have been produced largely from oil. This production is complex, costly and is not sustainable due to limited oil sources. The value that is addressed here is the ratio between the commercial price of butanol (1.2€ per kg) and its heat of combustion (10.80 kWh per kg) = 0.11€ per kWh relative to that of methane (≈0.15€ per kg):(15.42 kWh per kg) = 0.01€ per kWh.

At the end of their life cycle, most organic chemicals end up in the atmosphere as the greenhouse gas CO_2, the concentration of which is rapidly and continuously rising. Attempts are therefore being made to generate organic chemicals from CO_2 and water powered by renewable electricity as so-called 'artificial photosynthesis'[2–4]. However, relative to fossil fuels, renewable energy has a low energy density (for example, in Germany, installed renewable electric power generating 100 GW from a combination of photovoltaics (PV), windmills and biomass combustion is distributed over almost 400,000 square kilometres; https://www.energy-charts.de/power_inst_de.html). Therefore, it is necessary to decentralize industrial production of organic chemicals from CO_2 and water via electro-catalysis, to be smaller scale and to run with less chemical infrastructure[5–7]. By-product accumulation is typical, for example in the Fischer–Tropsch process[8], and thus elaborate separation techniques must also be avoided. This favours the involvement of microorganisms as they are often more selective than chemical catalysts to produce desired organic compounds. The Faradaic efficiency (efficiency of electron transfer into products) must be high in terms of converting all electricity into only the desired products. This favours the involvement of anaerobic microorganisms. If aerobic microorganisms are involved, a significant portion of the electrons can end up in water, increasing the electricity demand. Further, anaerobic fermenters are less expensive (there is less corrosion and in many cases sterilization is not required) than aerobic ones.

Herein, we describe the production of butanol and hexanol from CO_2, H_2O and renewable energy and how such a decentralized industrial plant with a capacity of a few 10,000 tonnes of butanol and/or hexanol per year might operate. A conventional PV module providing electricity with an energy conversion efficiency of around 20% (ref. [9]), a CO_2 electrolyser constantly operating at high current densities and a bioprocess module for the anaerobic conversion of CO, H_2 and CO_2 (syngas) to the desired alcohols were employed (Fig. 1 and Supplementary Fig. 1).

Results

Initial considerations. The CO_2 electrolyser in the hybrid system is the heart of this technical photosynthesis (Fig. 1) as it produces a mixture of mainly CO and H_2 (syngas of various composition) from electricity and CO_2 and H_2O. The lower redox potential of the CO/CO_2 couple ($E_0' = -520$ mV) as compared to that of the H^+/H_2 couple ($E_0' = -414$ mV) allows for anaerobic bacteria to perform a number of reduction reactions, such as reduction of carboxylic acids to their respective aldehydes ($E_0' = -580$ mV), or the reductive carboxylation of acetyl-CoA to pyruvate ($E_0' = -500$ mV). These reactions are thermodynamically and kinetically unfavourable; if H_2 was the sole electron donor in conjunction with CO_2 as the carbon source[10], practically no alcohols or pyruvate-derived products would be formed[11,12]. Therefore, the presence of CO is essential to gain the desired product selectivity.

For an industrial-scale electrochemical reduction, CO_2 concentrations higher than atmospheric concentrations are needed to produce larger concentrations of CO. Renewable sources of CO_2 include breweries, anaerobic digestion plants and power plants that convert biomass into electricity. CO_2 is also a side product of cement and steel production[13]. All of these CO_2 production sites are widely dispersed. CO_2 can also be concentrated from the atmosphere (0.04%) at a theoretical energy cost of at least 20 kJ mol^{-1}. Carbon capture from the atmosphere cannot be centralized because scrubbing out 1 mol CO_2 (44 g) requires at least 56,000 litres of air, which is another reason why industrial production of organic chemicals from CO_2 and H_2O should be decentralized.

[1]Evonik Creavis GmbH, Marl, Germany. [2]Siemens AG, Erlangen, Germany. [3]Covestro AG, Leverkusen, Germany. Ralf Krause and Martin Demler contributed equally to this work. *e-mail: guenter.schmid@siemens.com

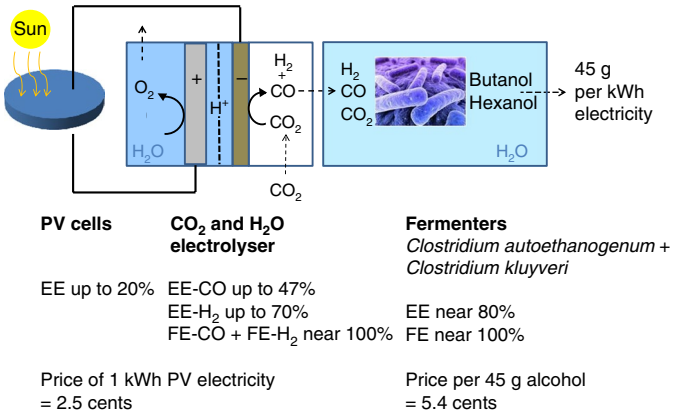

Fig. 1 | Sketch of the modules used in technical photosynthesis of 1-butanol and 1-hexanol from CO_2 and H_2O. For a detailed structure of the CO_2 electrolyser see Fig. 2a and for process design of the fermenters see Supplementary Fig. 1. PV, photovoltaic; EE, energy conversion efficiency; FE, Faradaic efficiency. Cents are 0.01€. At a PV-cell energy conversion efficiency of 20%, the overall energy conversion efficiency is above 8%. For calculation of the amount of butanol and hexanol obtained per kWh and for cost calculations see Methods. At present prices, the value of the alcohols formed is 2.2 fold higher than the price of the PV electricity consumed. Butanol costs 1.2€ per kg (ref. [1]). In the fermenters, syngas produced by the CO_2 electrolyser was converted first to acetate and ethanol by the anaerobic bacterium *Clostridium autoethanogenum*. Secondly, acetate and ethanol were fermented to butyrate and hexanoate by *C. kluyveri*; and thirdly, butyrate and hexanoate were reduced by CO and H_2 to butanol and hexanol, respectively, by *C. autoethanogenum*[60].

CO_2 electrolyser. In CO_2 electrolysers, CO_2 rather than HCO_3^- or CO_3^{2-} is reduced at a gas diffusion cathode[14]. Furthermore, CO_2 has a low solubility in salt-based electrolytes. Thus, the electric current density at the cathode's surface is generally too low for carrying out any technical applications (only a few mA cm^{-2}) when operating the electrolyser at a CO_2 pressure of 1 bar and ambient temperature[15–21], despite the fact that the Faradaic and energy conversion efficiencies are high[22,23]. We solved this problem by letting the gas diffusion cathode interact at its opposite side with 100% gaseous CO_2 rather than dissolved CO_2 (Fig. 2a). Covestro recently introduced such an operation mode in industrial chlorine–alkaline electrolysis called oxygen depolarization cathode (ODC) (cathode reaction: $½O_2 + H_2O + 2e^- \rightarrow 2OH^-$; anode reaction: $2Cl^- - 2e^- \rightarrow Cl_2$; https://www.covestro.com/en/sustainability/lighthouse-projects/sauerstoffverzehrkathode), which can work at electric current densities of more than 400 mA cm^{-2} (ref. [24]). There ODC was introduced to suppress the hydrogen evolution reaction (HER) and therefore decrease cell voltage and increase energy efficiency. Surprisingly, these commercially available gas diffusion electrodes also work in CO_2 electrolysis.

At this silver-based cathode, CO_2 was reduced to CO ($CO_2 + H_2O + 2e^- \rightarrow CO + 2OH^-$) and at the iridium-oxide-coated titanium anode[25,26], water was oxidized to O_2 ($H_2O - 2e^- \rightarrow ½O_2 + 2H^+$). In close proximity of the cathode, the pH becomes very basic ($CO_2 + H_2O + 2e^- \rightarrow CO + 2OH^-$), which in the bulk catholyte is neutralized by excess of CO_2 ($2OH^- + 2CO_2 \rightarrow 2HCO_3^-$). Thus, the overall cathode chamber reaction is: $3CO_2 + H_2O + 2e^- \rightarrow CO + 2HCO_3^-$. In other words, three CO_2 molecules have to be supplied to the gas diffusion electrode to accomplish electrochemical reduction of one CO_2.

The current–voltage characteristic of the CO_2 electrolyser (Fig. 2a) is depicted in Fig. 2b. The electric current density increased with increasing voltage and temperature. Extrapolation to zero current density yielded a minimal cell voltage of 2.3 V. The increase in current density was due to an increase in electrolyte conductivity when the temperature was raised from 30 °C to 60 °C.

At the silver-based gas diffusion electrode of the gas-to-gas CO_2 electrolyser (Fig. 2a), not all the CO_2 supplied could be converted to CO, and H_2 was competitively formed by proton reduction (HER). CO-Faradaic efficiency and H_2-Faradaic efficiency still totalled around 100%, because no other gaseous products were formed. The formation of traces of formic acid[27] can be neglected. The CO to H_2 ratio depends on the CO_2-supply rate (Fig. 2c and Table 1), because the rate of CO_2 reduction to CO at a given current density is kinetically limited by the diffusion of CO_2 to and CO from the cathode in the presence of a huge excess of H_2O. In contrast to most literature, our electrolysers were continuously operated far away from the thermodynamic limit to yield an industrially applicable current density. The maximum volumetric CO formation rate $\dot{V}_{CO_{max}}$ (l s^{-1}) is given by the total cell current I_{cell} (A)

$$\dot{V}_{CO_{max}} = \frac{V_{CO_{mol}}}{z \times F} \times I_{cell}$$

$\dot{V}_{CO_{max}}$ is the molar volume of CO (22.4 l mol^{-1}), F is the Faraday constant (96,485 A s mol^{-1}), and z is the number of electrons required to reduce CO_2 to CO, which is two. In order to characterize the operation conditions, we introduced the experimental parameter λ as the ratio of the volumetric CO_2 supply rate $\dot{V}_{CO_2}$ (l s^{-1}) and $\dot{V}_{CO_{max}}$

$$\lambda = \frac{\dot{V}_{CO_2}}{\dot{V}_{CO_{max}}}$$

Usually, $\lambda > 3$ is required to sufficiently reduce the competing HER. λ increases with increasing CO_2 flow rate and decreases with increasing electric current density. Furthermore, catholyte and anolyte are continuously mixed to ensure constant pH, K^+ and HCO_3^- concentration during the course of the long-term experiment.

At 300 mA cm^{-2} and a CO_2 flow rate of 90 sccm ($\lambda = 4.78$) the Faradaic efficiency for CO was near 70% and that for H_2 near 30% (Fig. 3a), and both remained almost constant within experimental error for more than 1,200 h (Fig. 3b) due to anolyte and catholyte mixing. Such high CO-Faradaic efficiencies at high current densities have in the past only been achieved for minutes under specific conditions, where in the electrolyser the electrolyte was cycled only once through the electrolysis cell and then discarded[18] or when electrocatalytic CO_2 reduction to CO was performed at high CO_2 pressure (>15 atm)[21].

The minimum cell voltage of 2.3 V (Fig. 2b) corresponds to a theoretical maximum total ($CO + H_2$) energy efficiency of 64%, assuming an adiabatic cell potential of 1.47 V (for calculation see Methods). With increasing current density the CO energy conversion efficiency decreased (Fig. 3a). At 300 mA cm^{-2}, the total energy efficiency for CO and H_2 dropped to nearly 20%. Therefore, when CO:H_2 ratios lower than around 2:1 (Fig. 3b) are anticipated, it is more energy efficient to use in parallel a separate H_2O electrolyser rather than to increase the electric current density in the CO_2 electrolyser. H_2O-electrolysers operate stably at electric current densities of, for instance, 1.5 A cm^{-2} at around 2 V with an energy efficiency of around 70% (ref. [28]).

The syngas collected was almost free of O_2 (≪100 ppm), because the catholyte was separated from the site of CO_2 reduction by the gas diffusion electrode. Any O_2 diffusing into the cathode from the front side or dissolved in the electrolyte was reduced to OH^- (ODC reaction), which reacted with CO_2 to form HCO_3^- (Fig. 2a). The concentration of this O_2 was very low, as can be deduced from the Faradaic efficiency of CO_2 and H_2O reduction to CO and H_2, respectively, which was found to be nearly 100%. Very low O_2 concentrations in the out-coming

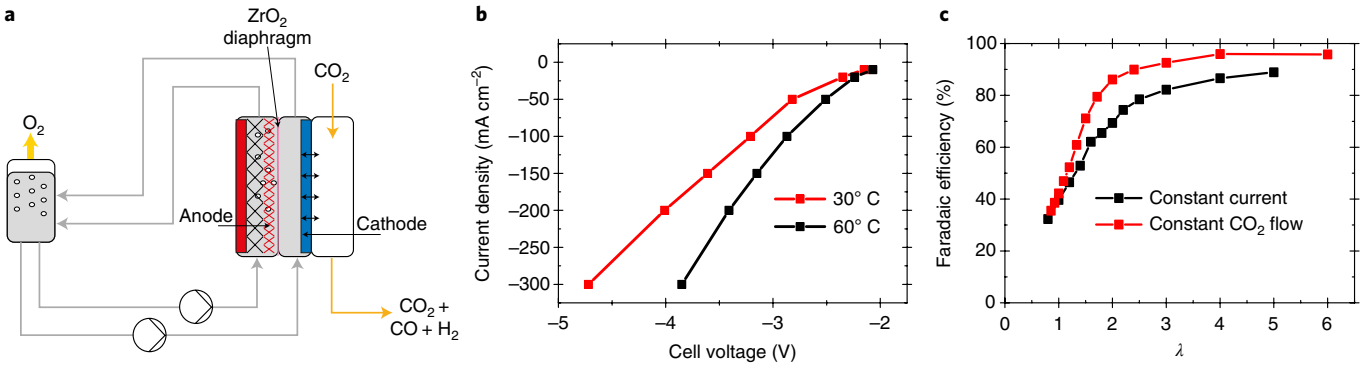

Fig. 2 | Scheme and properties of the CO_2 electrolyser. a, The cathode was a silver-based gas diffusion electrode and the anode an iridium-oxide-coated titanium anode with a zero-gap structure. CO_2 was allowed to flow only at the electrolyte opposite the cathode with an effective surface area of 10 cm^2. The anolyte and the catholyte solutions, both 0.1 M K_2SO_4/1.5 M $KHCO_3$ (pH ≈ 7), were continuously cycled and mixed at a flow rate of 200 ml min^{-1}. The temperature was 30 °C. The cathode and the anode were 2 mm apart and separated by a high-conductivity, zirconium-oxide-based diaphragm. **b**, Dependence of the electric current density on the voltage and temperature. The CO_2 flow rate was 10.5 sccm (standard cubic centimetre per min). **c**, Faradaic efficiency of CO summarized from the data given in Table 1.

syngas are of importance, as higher concentrations are toxic for the bacteria converting the syngas to butanol and hexanol in the fermentation phase.

Table 1 | Dependence of the CO Faradaic efficiency (FE-CO) on the experimental variables

CO_2 flow (sccm)	λ	FE-CO (%)	U_{cell}(V)
Constant current density J = 150 mA cm^{-2}			
52.5	5	88.9	4.91
42	4	86.6	4.91
31.5	3	82.2	4.92
26.25	2.5	78.5	4.93
23.1	2.2	74.4	4.93
21	2	69.4	4.93
18.9	1.8	65.5	4.94
16.8	1.6	62.1	4.94
14.7	1.4	52.9	4.95
12.6	1.2	46.5	4.95
10.5	1	39.7	4.96
8.4	0.8	32.3	4.96
J (mA cm^{-2})	**λ**	**FE-CO (%)**	**U_{cell}(V)**
Constant CO_2 flow at 10.5 ml min^{-1}			
25	6	95.8	2.66
37.5	4	96.0	3.11
50	3	92.6	3.45
62.5	2.4	90.0	3.75
75	2	86.1	4.01
87.5	1.71	79.5	4.23
100	1.5	71.1	4.38
112.5	1.33	60.9	4.52
125	1.2	52.3	4.67
137.5	1.09	46.9	4.81
150	1	42.2	4.97
175	0.86	35.5	5.30

The dependence of the CO Faradaic efficiency (FE-CO) on the CO_2 supply rate, on the electrical current density and on λ (for definition see text). The cathode and the anode were 9.5 mm apart and separated by a high-conductivity, zirconium-oxide-based diaphragm.

During development of the CO_2 electrolyser described above we first experimented with a preliminary operational mode shown and described in Supplementary Fig. 2a. The main differences were independent electrolyte cycling and H_2SO_4 as anolyte. At current densities of 50 mA cm^{-2}, this CO_2 electrolyser also generated CO at high Faradaic efficiency for more than 1,000 h (Supplementary Fig. 3), but the CO Faradaic efficiency decreased more with increasing current density than in the setup shown in Fig. 2a. We coupled this preliminary CO_2 electrolyser with a commercially available PV module and measured the power dependence on the voltage for the coupled system (Supplementary Fig. 4). The two curves intersected near 2.8 V and a power near 1.5 W, corresponding to a current density of about 0.5 A per 10 cm^2. At the intersection point, solar module and CO_2 electrolyser were optimally coupled and didn't require extensive regulation.

Reference electrodes, which would have allowed determination of the rate-limiting electrode, were not included in our devices, because we wanted to work at high current densities and, thus, with a very high gas load. At high current densities, conductivity of the electrolyte becomes one major contribution to energy losses, which can be roughly calculated from the distance between anode and cathode and the corresponding cell voltage (Figs. 2 and 3). CO_2 evolution (gas bubbles) on the anode side might be another loss channel (see Methods).

Conversion of syngas to acetate and ethanol. In a first experiment, syngas was produced by the PV-module-powered CO_2 electrolyser at a rate of 16.52 sccm and a composition of 11.76 % CO (4.8 mmol h^{-1}), 6.37 % H_2 (2.6 mmol h^{-1}) and 81.86 % CO_2 (33.4 mmol h^{-1}). This mixture was fed into two 1-litre fermenters, each with 0.5 litre culture at 36 °C, in which CO, H_2 and CO_2 were converted to acetate (reaction (1)) and ethanol (reaction (2)) by the activity of *C. autoethanogenum*[11,29–32]. The acetogen can, like the closely related *C. ljungdahlii*, grow mixotrophically[33] and is amenable to genetic modification[12,29].

$$4H_2 + 2CO_2 \rightarrow CH_3COO^- + H^+ + 2H_2O \quad (1)$$

$\Delta G^{0\prime} = -94.6$ kJ mol^{-1}; $\Delta H^{0\prime} = -310.3$ kJ mol^{-1}

$$CH_3COO^- + H^+ + CO + H_2 \rightarrow CH_3CH_2OH + CO_2 \quad (2)$$

$\Delta G^{0\prime} = -29.7$ kJ mol^{-1}; $\Delta H^{0\prime} = -34.3$ kJ mol^{-1}

After 50 h of cell growth, stationary conditions were reached, where the cell concentration, the rates of CO and H_2 consumption

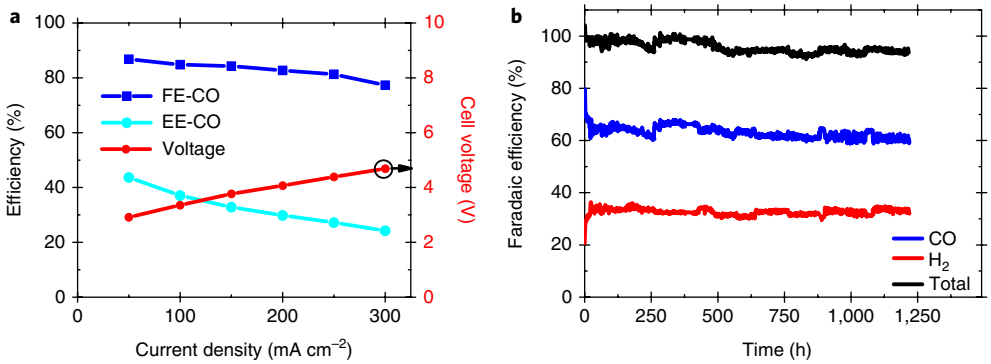

Fig. 3 | Further properties of the CO_2 electrolyser shown in Fig. 2a. a, Dependence of Faradaic efficiencies (FE) and energy conversion efficiencies (EE) on the electric current density (conditions as in Fig. 2a). The anolyte and the catholyte solutions, both 0.1 M K_2SO_4/1.5 M $KHCO_3$ (pH ≈ 7), were continuously cycled and mixed at a flow rate of 200 ml min^{-1}. The temperature was 30 °C. The gas diffusion electrode was operated at $\lambda = 4.3$, which corresponded to a CO_2 flow-rate of 90 sccm. **b**, Stability of the CO-FE and H_2-FE at an electric current density of 300 mA cm^{-2}. The cell voltage stayed constant within 7.0–7.5 V during the course of the experiment. The cathode and the anode were 9.5 mm apart and separated by a high-conductivity, zirconium-oxide-based diaphragm. The anolyte and the catholyte solutions, both 0.4 M K_2SO_4/0.5 M $KHCO_3$ (pH ≈ 7), were continuously cycled and mixed at a flow rate of 200 ml min^{-1}. The temperature was 30 °C. The gas diffusion electrode was operated at $\lambda = 4.78$, which corresponded to a CO_2 flow-rate of 100 sccm. H_2, CO and CO_2 concentrations were measured every 12 min.

and those of acetate and ethanol formation remained substantially constant for the next 45 h. The consumed CO and H_2 (3.35 mmol h^{-1} in total) agreed well with the mol electron pairs (3.44 mmol h^{-1}) required to reduce CO_2 to acetate and ethanol (Table 2). The Faradaic efficiency (here the expression Faradaic efficiency is analogous to the characterization of the electrolyser) was almost 100%, indicating that essentially only acetate and ethanol were formed under the experimental conditions. The efficiency of energy conversion in syngas fermentation, calculated from the amount of ethanol produced (reactions (1) + (2)), was almost 80% (see Methods). Considering that the energy conversion efficiency of the CO_2 electrolyser at a low electric current density of about 50 mA cm^{-2} was nearly 50% (Fig. 2c) and that of existing PV modules can be nearly 20%, the overall energy conversion efficiency of the described artificial photosynthesis system can be as high as 8% (Fig. 1). Similarly high conversion efficiencies have recently been described for a hybrid water splitting biosynthetic system involving *Ralstonia eutropha* for the reduction of CO_2 with H_2 to fuel alcohols[34,35], albeit at much lower electric current densities. An integrated electromicrobial conversion of CO_2 via formate to higher alcohols using recombinant *R. eutropha* strains also proceeded only at low current densities[36].

Besides acetate and ethanol, *C. autoethanogenum* is known to produce small amounts of 2,3-butanediol and lactic acid[29]. These side products were, however, only formed in significant amounts when the CO concentration and the CO:H_2 ratio in the syngas were much higher.

Conversion of syngas to butanol and hexanol. In a second experiment, the CO_2 electrolyser was run at an electric current density of 150 mA cm^{-2} (Supplementary Fig. 3b), resulting in a constant syngas production at a flow rate of 16.23 sccm and composition of 10% CO (4 mmol h^{-1}), 60% H_2 (24.2 mmol h^{-1}) and 30% CO_2 (12.2 mmol h^{-1}).

Again the syngas was fed into two 1-litre fermenters each with 0.5 litre *C. autoethanogenum* culture. 22 h later, the fermenters were additionally inoculated with *C. kluyveri* cells. At the point of addition, the fermenter already contained acetate and ethanol, formed from CO, H_2 and CO_2 by the activity of *C. autoethanogenum* (reactions (1) and (2)). This inoculation led to the acetate and ethanol being converted to butyrate (reaction (3)) and hexanoate (reaction (4)) by *C. kluyveri*[37,38] and then to butanol (reaction (5)) and hexanol (reaction (6)) by *C. autoethanogenum*[10,39–42].

$$CH_3COO^- + CH_3CH_2OH \rightarrow CH_3CH_2CH_2COO^- + H_2O(C.\ kluyveri) \quad (3)$$

$$CH_3CH_2CH_2COO^- + CH_3CH_2OH \rightarrow CH_3CH_2CH_2CH_2CH_2COO^- + H_2O(C.\ kluyveri) \quad (4)$$

$$CH_3CH_2CH_2COOH + CO + H_2 \rightarrow CH_3CH_2CH_2CH_2OH + CO_2(C.\ autoethanogenum) \quad (5)$$

$$CH_3CH_2CH_2CH_2CH_2COOH + CO + H_2 \rightarrow CH_3CH_2CH_2CH_2CH_2CH_2OH + CO_2(C.\ autoethanogenum) \quad (6)$$

After steady state conditions were reached, the rates of CO and H_2 consumption and those of acetate and ethanol formation remained substantially constant for 45 h. The consumed CO and H_2

Table 2 | Acetate and ethanol formation by *C. autoethanogenum* from H_2, CO and CO_2 produced by the CO_2 electrolyser that was powered by electricity from a PV module

	H_2	CO	$\Sigma H_2 + CO$	C_2OOH	C_2OH	ΣC_2
H_2 and CO consumed and products formed (mmol h^{-1})	0.99	2.36	3.35	0.81	0.035	
Electron pairs recovered in products (mmol h^{-1})				3.24	0.21	3.44

50 h after inoculation of the fermenters with *C. autoethanogenum*, the cell concentration and the rates of gas consumption and of product formation were constant for at least 48 h thereafter. The rates within these 48 h were averaged. For details (time course, cell density, product distribution and substrate consumption rates) see Methods.

(14.88 mmol h^{-1} in total) agreed well again with the mol electron pairs (14.52 mmol h^{-1}) required to reduce CO_2 to the three acids and alcohols (Table 3). The Faradaic efficiency was close to 100%. The energy conversion efficiency of formation of butanol and hexanol from CO, H_2 and CO_2 was nearly 78% (see Methods).

Interestingly, *C. carboxidovorans* alone can catalyse reactions (1)–(6)[12,40]. However, the growth rate (0.023 h^{-1}) of this acetogen is far too low for a technical process.

Process design. As shown in Table 3, the conversion of CO, H_2 and CO_2 into butanol and hexanol can take place in a mixed culture of *C. autoethanogenum* and *C. kluyveri* under non-growth conditions. For an industrial process, however, it is important that the conversion takes place under chemostat (continuous) conditions and in two separate fermenters, as the optimum performance conditions of *C. autoethanogenum* and *C. kluyveri* differ. This is the basis for the design of an industrial process, forming butanol and hexanol at a scale of 10,000 tonnes per year (Supplementary Fig. 1). A prerequisite for a technical process is that the rate of carbon atoms being fixed in the gas fermenter is the same as the rate of carbon atoms being transformed to butanol and hexanol. For continuous fermentation, accumulation of the intermediates acetic acid and ethanol, as well as butyric acid and hexanoic acid, should be avoided. Here, we have shown experimentally that this prerequisite can be fulfilled (Supplementary Table 1).

To calculate the necessary current, pentanol is used as an example because it represents a 1:1 mixture of hexanol and butanol. Around 3.4×10^9 mol electrons are required to synthesize 10,000 tonnes pentanol. This means 328×10^{12} coulomb per year or 10.4×10^6 A (1 A = 1 C s^{-1}). At a minimal CO to H_2 consumption ratio of 1/5 in the fermentation (see reactions (9) and (10) in Methods), 16.7% of these electrons must be provided by the CO_2 electrolyser. It would possess a power of 8.2 MW (4.7 V × 1.74×10^6 A), assuming a supply voltage of 4.7 V (Fig. 2b). The remaining 83.3% of the required electrons are provided by the H_2O electrolyser, which at around 2.0 V, for example, would have to run at a power of 17.3 MW (2.0 V × 8.66×10^6 A). The overall plant would therefore consume 8.2 MW + 17.3 MW = 25.5 MW. This power could be provided by 14.6×10^4 m^2 = 14.6 hectare PV modules with power density values of 175 W m^{-2}. Taking into account night-time, location and weather of the hypothetical plant, an area 5–10 times larger would be required (https://en.wikipedia.org/wiki/List_of_photovoltaic_power_stations).

For the example of the production of 10,000 tonnes of the alcohols, 568×10^6 mol (that is, 25,000 tonnes) of CO_2 are required. The CO_2 has to be fed into the CO_2 electrolyser at a rate of 1.1×10^3 mol min^{-1}, which is equal to a flow rate of 24.6×10^6 sccm (100% CO_2 at 10^5 Pa). At 4.7 V (30 °C) and a λ of 4.3, the input CO_2 flow rate of our CO_2 electrolyser was 90 sccm (Supplementary Fig. 3). Therefore, the CO_2 electrolyser would have to be scaled up by a factor of 270,000. This can be achieved by increasing the electrode surface area from 10 cm^2 to 1 m^2 (factor 10^3) and by stacking 270 electrolysis cells. Both of which in principle are possible and are being done.

In the fermenters, butanol and hexanol were produced together at a rate of 0.6×10^{-3} mol per hour per litre of culture (Supplementary Table 1). For the production of 10,000 tonnes of butanol and hexanol per year (that is, 12.9×10^3 mol alcohol per hour), the fermenters would have to be scaled up by a factor of 21.6×10^6. This scale-up may be achieved by increasing the cell concentration in the fermenters by a factor of up to 30 and the volume from 1 litre to 700,000 litres, a volume not unusual in industrial fermentations[43–47]. At this large volume it is advantageous that *C. autoethanogenum* and *C. kluyveri* grow in the fermenters in media containing only vitamins and minerals. The highly selective conditions make sterilization of the media unnecessary. This is especially important because it significantly reduces investment costs.

Another advantage of this set-up is that the products, butanol and hexanol, are easily extracted, allowing the unused media components to be easily recycled, which reduces the costs of water and media components. Butanol and hexanol are separated in two steps from the aqueous broth. The first step is to extract the alcohols using oleyl alcohol as an extracting solvent. The second step is to separate the alcohols from the solvent by distillation and recycle the solvent. The main energy consumption of this separation is the distillation step. To vaporize hexanol, 0.16 kWh kg^{-1} is needed, because of the vaporization enthalpy of 60 kJ mol^{-1}. In addition, the solvent has to be heated up to its vaporization temperature. This heat can only partly be recovered. Therefore, in sum roughly 0.6 kWh kg^{-1} hexanol energy is required to separate the products. This can be neglected compared to the energy consumed to synthesize the molecules, which is roughly 22 kWh kg^{-1} alcohol.

The advantages discussed above and the anticipated future low electricity costs (Fig. 1) all contribute to making this relatively small-scale approach competitive with traditional high-scale chemical productions of butanol and hexanol.

Under the experimental conditions described, butanol and hexanol were produced at almost the same rate (Supplementary Table 1). However, the ratio can be tuned, since it depends on the acetate to ethanol ratio[48], which in turn depends on the CO/H_2 ratio in the syngas[29]. This is important since at present the butanol market[1] is larger than the hexanol market[49], but this may vary in future. Hexanol, apart from its present direct use in perfumes and other cosmetic applications, can be chemically dehydrated to 1-hexene[50] which is an important co-monomer for the production of polyethylene. Since hexanol is a liquid, it can also be easily transported to any polyethylene producer. Furthermore, hexanol could immediately substitute gasoline from fossil sources.

Other microorganisms can be combined with *C. autoethanogenum* instead of *C. kluyveri*, namely *Pelobacter propionicus*[51], which ferments ethanol plus CO_2 to propionate and acetate or oleaginous yeast[52], which convert ethanol and acetate to lipids. The right combination allows the production of various platform chemicals via artificial photosynthesis involving CO_2 electrolysis, as described here, at high Faradaic efficiencies.

Table 3 | Formation of acetate (C_2OOH), ethanol (C_2OH), butyrate (C_4OOH), butanol (C_4OH), hexanoate (C_6OOH) and hexanol (C_6OH) from H_2, CO and CO_2 by *C. autoethanogenum* plus *C. kluyveri*

	CO	$\Sigma H_2 + CO$	C_2OOH	C_2OH	C_4OOH	C_4OH	C_6OOH	C_6OH	$\Sigma C_{2,4,6}$
H_2 and CO consumed and products formed (mmol h^{-1})	2.08	14.88	1.45	0.6	0.21	0.14	0.05	0.04	
Electron pairs recovered in products (mmol h^{-1})			5.8	3.6	2.1	1.68	0.8	0.72	14.7

22 h after inoculation of the two fermenters with *C. autoethanogenum*, cells of *C. kluyveri* were added. 6 h later the rates of gas consumption and of product formation were found to be constant for at least 24 h (for details see text). The rates within these 24 h were averaged. For details (time course, cell density, product distribution and substrate consumption rates) see Methods.

Methods

The results reported above are examples. They are backed up, however, by many additional experiments performed under almost identical or very similar conditions leading to the same results.

Free energy and enthalpy changes are given under standard conditions: CO, H_2 and CO_2 as gas at 10^5 Pa and acetate, ethanol, butyrate, hexanoate, butanol and hexanol at 1 molal solution.

The microfiltration system to retain the acetogenic cells in the gas fermenter (Supplementary Fig. 1) was developed for the improved fermentation of gaseous substrates[53].

Photovoltaic module. In our experiments the silicon PV modules were irradiated with a solar simulator with 1,000 W m^{-2}, simulating conditions on a sunny day with an air mass coefficient of 1.5 (standard test conditions). The temperature of the PV module was kept constant at 25 °C by a Peltier element. PV module (12.8 × 12.8 cm^2 = 164 cm^2), from Conrad Electronics, consisted of 32 PV cells (1.7 × 2.6 cm^2), each eight connected in series. At the maximum power point (1.8 W; Supplementary Fig. 4), the PV module delivered 482 mA per 10 cm^2 at 3.7 V and operated at a solar energy conversion efficiency of 11% (1.8 W × 100% / 16.4 W).

CO_2 electrolyser. Commonly, in CO_2 electrolysers the anolyte and catholyte contain mostly $KHCO_3$ at a pH around 7. The anolyte and catholyte are separated by a Nafion membrane. Due to the concentration difference of protons (10^{-7} M) and potassium cations (10^{-1} M), the Nafion membrane is mostly potassium conducting. This leads to the following catholyte reaction: $3CO_2 + H_2O + 2e^- \rightarrow CO + 2HCO_3^-$. With the potassium ions from the anolyte, the catholyte concentration of $KHCO_3$ increases proportional to the charge flow until precipitation. The anolyte reactions are as follows: $H_2O - 2e^- \rightarrow ½O_2 + 2H^+$ and $2HCO_3^- + 2H^+ \rightarrow 2CO_2 + 2H_2O$. The concentration of $KHCO_3$ decreases proportional to the charge flow until all of the potassium cations have moved to the catholyte and only water is left as anolyte. To overcome this problem, two operation modes were tested: (i) in Supplementary Fig. 2a an almost continuous operation mode with sulfuric acid as the anolyte and $KHCO_3$ as the catholyte separated by a Nafion membrane is shown. Both anolyte and catolyte are running in separated cycles. However, with each proton, about four molecules of water are pulled through the membrane, which leads to a concentration of sulfuric acid in the anolyte and a dilution of $KHCO_3$ in the catholyte. (ii) The final solution is described schematically in Fig. 2a. In this set-up a mixture of $KHCO_3$ and K_2SO_4 is used both as catholyte and anolyte, which are mixed after each cycle with the result that cations, anions, pH and water remain balanced. A Nafion membrane is no longer needed and is replaced by a ZrO_2 diaphragm. Only the latter set-up is described here in more detail.

A commercial silver-based gas diffusion electrode (GDE) from Covestro, typically used as an oxygen depolarized cathode (ODC) in chloralkaline electrolysis[24,54], was used as cathode. The silver-based cathode is sensitive to H_2S (ref. [55]) and other contaminants present in CO_2 obtained from cement and steel production, alcohol formation in breweries, anaerobic digestion plants and power plants converting biomass into electricity. Therefore, the CO_2 has to be freed of these contaminants before being used in the CO_2 electrolyser.

As anode, an Ir-MMO (iridium-mixed metal oxide) coated titanium sheet was used[25,26], which was purchased with the flow cell from ElectroCell. Such anodes are typically used in PEM type electrolysers (polymer / proton exchange membrane) for hydrogen production.

The aqueous catholyte and anolyte consisted of mixtures of $KHCO_3$ and K_2SO_4 (see captions of Figs. 2 and 3) at pH 7 without further additives. The conductivity was about 0.13 S cm^{-1}, which is low compared to alkaline hydrogen electrolyses (~1 S cm^{-1}). In CO_2 electrolysis, highly conductive catholytes like bases or acids cannot be used. While acids tend to form only H_2 at the cathode due to the high proton concentration, bases like KOH lead to the formation of CO_3^{2-} and HCO_3^-. Neither can be reduced at the cathode and may form the salts K_2CO_3 or $KHCO_3$, which tend to crystallize and thus clog the GDE.

The electrolyte solutions were prepared with ultra-pure water (18.2 MOhm cm at 273 K, MilliQ Millipore system). Potassium hydrogen carbonate, potassium sulfate and sulfuric acid were used without further purification and were purchased from Alfa Aesar. All experiments were conducted by pre-saturating the electrolyte with CO_2 for 30 min.

All electrochemical experiments were conducted in a flow cell, which was purchased by ElectroCell (Micro Flow Cell) and slightly modified. This flow cell is a sandwich of three compartments with two liquid channels containing the catholyte and anolyte, and one CO_2 gas channel behind the cathode. The anode and the cathode compartments are separated by a ZrO_2 diaphragm. The surface area of each electrode was 10 cm^2. CO_2 gas (4.8 Linde) was used without further purification and continuously supplied at a constant flow rate controlled by a mass flow controller (Bronkhorst F-200CV-002-AAD-33-V) at atmospheric pressure. The flow rates are shown in the corresponding graphs.

A peristaltic pump (Ismatec ECOLINE VC-MS/CA8-6) was used to supply the electrolyte between the anode and GDE cathode at a flow rate of 200 ml per min. The flow rate had only minor effects on the CO Faradaic efficiency. The electrolyte reservoirs were magnetically stirred glass flasks held at a constant temperature (30 °C) using a hot plate in combination with a glass-covered contact thermometer in the electrolyte. Contact between the electrolyte and any metal components was avoided to exclude contamination and a possible deactivation of the silver-based catalyst. These glass flasks were used for gas separation from the electrolyte. Contaminated GDEs form predominantly H_2.

The electrochemical flow reactor was operated using a potentiostat (Metrohm Autolab PGSTAT-30 with BOOSTER20A) under ambient pressure and temperature. Experiments were carried out in galvanostatic conditions, where a constant current is applied and the required voltage is monitored.

Conversion efficiency of the CO_2 electrolyser. The theoretical minimal cell voltage for the electrolysis of CO_2 to CO and O_2 is 1.34 V when calculated from $\Delta G^0 = -258.5$ kJ mol^{-1} of the reaction: $CO_2(g) \rightarrow CO(g) + ½O_2(g)$ or from the redox potential difference $E_0' = +0.82$ V of the $O_2/2H_2O$ couple and $E_0' = -0.52$ V of the CO_2/CO couple[56]. Thus, at 3.65 V, the operation voltage of the CO_2 electrolyser when coupled to the PV module, electrolysis theoretically proceeds at an over potential of 2.3 V with an energy conversion efficiency of 37%. However, it is better to consider $\Delta H^{0'} = -283.2$ kJ mol^{-1} of the reaction, which corresponds to an adiabatic minimal cell potential of 1.47 V. Otherwise an external heat source is needed to compensate an entropy increase. This limits the efficiency of the setup to 40% when 3.65 V is applied.

In the CO_2 electrolyser the distance between cathode and anode was 2 mm, which—depending on the electric current density—led to a significant ohmic loss. Ohmic losses were less at 60 °C than at 30 °C due to the higher conductivity of the electrolyte (Fig. 2b and Supplementary Fig. 2b).

Growth media. Medium A for *C. autoethanogenum* contained per litre composition: 1 g NH_4Cl, 0.1 g KCl, 0.2 g $MgSO_4 \cdot 7H_2O$, 0.8 g NaCl, 0.1 g KH_2PO_4, 20 mg $CaCl_2 \cdot 2H_2O$, 0.4 g L-cysteine-HCl, 0.4 g $Na_2S \cdot 9H_2O$, 20 mg nitrilotriacetic acid, 10 mg $MnSO_4 \cdot H_2O$, 8 mg $(NH_4)_2Fe(SO_4)_2 \cdot 6\ H_2O$, 2 mg $CoCl_2 \cdot 6\ H_2O$, 2 mg $ZnSO_4 \cdot 7H_2O$, 0.2 mg $CuCl_2 \cdot 2H_2O$, 0.2 mg $Na_2MoO_4 \cdot 2H_2O$, 0.2 mg $NiCl_2 \cdot 6H_2O$, 0.2 mg Na_2SeO_4, 0.2 mg $Na_2WO_4 \cdot 2H_2O$, 20 µg biotin, 20 µg folic acid, 100 µg pyridoxine-HCl, 50 µg thiamine-HCl · H_2O, 50 µg riboflavin, 50 µg nicotinic acid, 50 µg Ca-pantothenoic acid, 1 µg vitamine B_{12}, 50 µg *p*-aminobenzoic acid, 50 µg lipoic acid and 1 g yeast extract. The pH was adjusted to the pH indicated under continuous gassing.

Medium B for *C. autoethanogenum*, which differed from medium A mainly in not containing yeast extract, contained per litre compostion: 0.5 g $MgCl_2 \cdot 6H_2O$, 0.21 g NaCl, 0.135 g $CaCl_2 \cdot 2H_2O$, 2.65 g $NaH_2PO_4 \cdot 2H_2O$, 0.5 g KCl, 2.5 g NH_4Cl, 15 mg nitrilotriacetic acid, 30 mg $MgSO_4 \cdot 7H_2O$, 5 mg $MnSO_4 \cdot H_2O$, 1 mg $FeSO_4 \cdot 7H_2O$, 8 mg $Fe(SO_4)_2(NH_4)_2 \cdot 6H_2O$, 2 mg $CoCl_2 \cdot 6H_2O$, 2 mg $ZnSO_4 \cdot 7H_2O$, 200 µg $CuCl_2 \cdot 2H_2O$, 200 µg $KAl(SO_4)_2 \cdot 12H_2O$, 3 mg H_3BO_3, 300 µg $Na_2MoO_4 \cdot 2H_2O$, 200 µg Na_2SeO_3, 200 µg $NiCl_2 \cdot 6H_2O$, 200 µg $Na_2WO_4 \cdot 6H_2O$, 20 µg D-biotin, 20 µg folic acid, 10 µg pyridoxine-HCl, 50 µg thiamine-HCl, 50 µg riboflavin, 50 µg nicotinic acid, 50 µg Ca-pantothenate, 50 µg vitamin B_{12}, 50 µg *p*-aminobenzoate, 50 µg lipoic acid, 10 mg $FeCl_3$ with additional 500 mg L-cysteine-HCl. The pH was adjusted to 6 under continuous gassing.

Medium C for *C. kluyveri* contained per litre compostion: 0.25 g NH_4Cl, 0.2 g $MgSO_4 \cdot 7H_2O$, 0.31 g K_2HPO_4, 0.23 g KH_2PO_4, 2.5 g $NaHCO_3$, 1 g yeast extract, 10 g K-acetate, 20 g ethanol, 0.25 g L-cysteine-HCl, 1.5 mg $FeCl_2 \cdot 4H_2O$, 70 µg $ZnCl_2 \cdot 7H_2O$, 100 µg $MnCl_2 \cdot 4H_2O$, 6 µg boric acid, 190 µg $CoCl_2 \cdot 6H_2O$, 2 µg $CuCl_2 \cdot 6H_2O$, 24 µg $NiCl_2 \cdot 6H_2O$, 36 µg $Na_2MoO_4 \cdot 2H_2O$, 3 µg $Na_2SeO_3 \cdot 5H_2O$, 4 µg $Na_2WO_4 \cdot 2H_2O$, 100 µg vitamine B12, 80 µg *p*-amino-benzoic acid, 20 µg biotin, 200 µg nicotinic acid, 100 µg Ca-pantothenoic acid, 300 µg pyridoxine-HCl, 200 µg thiamine-HCl · H_2O. The pH was adjusted to 7.5.

Conversion of syngas to acetate and ethanol. *C. autoethanogenum* (DSMZ 10061, Braunschweig) was routinely grown at 37 °C under continuous gassing with 67% H_2 and 33% CO_2 on medium A containing additionally 20 g l^{-1} MES (adjusted to pH 6.0). The medium was then inoculated per litre with 100 ml of an active pre-culture grown to an OD_{600} of 0.5 on the same medium. At an OD_{600} of about 0.5, the cells were anaerobically harvested by centrifugation and the cell pellet from 100 ml culture re-suspended in 1 ml medium and the suspension then used to equally inoculate two 1 litre fermenters (run in series) each containing 500 ml of medium A and continuously gassed with syngas from the CO_2 electrolyser at a rate of 16.52 sccm and a composition of 11.76% CO (4.8 mmol h^{-1}), 6.37% H_2 (2.6 mmol h^{-1}) and 81.86% CO_2 (33.4 mmol h^{-1}).

In fermenter-1 the pH was kept constant at 5.5 and in fermenter-2 at 6.0 by the continuous addition of a base (anaerobic potassium hydroxide, 140 g l^{-1}) with a peristaltic pump. After 50 h of growth, the OD_{600} in fermenter-1 increased from 0.05 to 1.3 and in fermenter-2 from 0.05 to 1.1 to then remain essentially constant for the next 45 h. In these 45 h, the flow rate of the gas coming out of the fermenters (16.03 sccm) and its composition of 6.03% CO (2.44 mmol h^{-1}), 3.96% H_2 (1.61 mmol h^{-1}) and 90.00% CO_2 (36.4 mmol h^{-1}) remained substantially constant, indicating a constant conversion rate of syngas into acetate and ethanol (Table 2).

Conversion of syngas to butanol and hexanol. The experimental setup was identical to that described for Table 2, except for the fact that the CO_2 electrolyser was powered at 5.4 V, resulting in an electric current density of 150 mA cm^{-2}.

At that time, cells of *C. kluyveri* (DSMZ 555, Braunschweig) were added and in medium A (see section 'Growth media') 20 g MES per litre was additionally present. The two 1-litre fermenters (run in series), each containing 500 ml medium, were gassed with 10% CO (4 mmol h^{-1}), 60% H_2 (24.2 mmol h^{-1}) and 30% CO_2 (12.2 mmol h^{-1}) from the CO_2 electrolyser at a flow rate of 16.23 sccm and then inoculated in equal parts with *C. autoethanogenum* cells harvested from 80 ml of an actively growing syngas culture (OD_{600} = 0.62). After 22 h, the fermenters were additionally inoculated in equal parts with *C. kluyveri* cells harvested from 60 ml of a culture (OD_{600} = 0.86) growing on ethanol and acetate. Six hours after the addition of the *C. kluyveri* cells, the rates of gas consumption and of product formation remained substantially constant for at least 24 h. In these 24 h, the flow rate of the outcoming gas (8.35 sccm) and its composition of 9.6% CO (2.0 mmol h^{-1}), 54% H_2 (11.3 mmol h^{-1}) and 36.4% CO_2 (7.6 mmol h^{-1}) remained substantially constant.

C. kluyveri was routinely grown on ethanol and acetate at 36 °C in medium C. The pH was adjusted to 7.5 and the medium then inoculated to an OD_{600} of 0.1 with an actively growing pre-culture in the same medium. At OD_{600} = 0.86, the cells from 60 ml of culture were anaerobically harvested by centrifugation and the cell pellet re-suspended in 10 ml of anoxic medium C and equal parts of the suspension used to inoculate the two fermenters.

Gas analysis. The product gases from the CO_2 electrolyser were measured with a Thermo Scientific Trace 1310 gas chromatograph (GC) equipped with two thermal conductivity detector (TCD) channels. The GC is directly connected to the experiment via a heated transfer line. For separation of CO_2, O_2, CO and hydrocarbons, a micropacked GC column (shin carbon) was used with He as carrier. The determination of H_2 was performed on a packed mol-sieve column using Ar as carrier. In the product gases from the cathode only CO and H_2 were detected by GC when using Ag as the catalyst. No traces of hydrocarbons (GC calibrated for CH_4, C_2H_4, C_2H_2, C_2H_6 down to 20 ppm) were detected. The cycle time of the GC was 12 min. The GC was calibrated biweekly. In relation to the fermenters, gas samples were taken before the first fermenter inlet and after the last fermenter gas outlet.

Solute analysis. Liquid samples were taken from the cultures via the sampling port of the fermenters and concentrations of acetate, butyrate, hexanoate, ethanol, butanol and hexanol were determined by quantitative ^{1}H NMR spectroscopy (Bruker AVANCE III HD, 600 MHz). Prior to quantitative analysis, samples were diluted with an adequate amount of phosphate buffer containing the internal standard trimethylsilyl propionate.

Calculation of energy conversion efficiencies. The energy conversion efficiency of the syngas fermentation to ethanol was calculated from the enthalpy changes ($\Delta H^{0'}$) associated with reactions (1) and (2) and those associated with the combustion of H_2 (reaction (7)) and CO (reaction (8)).

$$2H_2 + O_2 \rightarrow 2H_2O \quad (7)$$

$\Delta G^{0'} = -474.3$ kJ mol^{-1}; $\Delta H^{0'} = -571.7$ kJ mol^{-1}

$$2CO + O_2 \rightarrow 2CO_2 \quad (8)$$

$\Delta G^{0'} = -514.4$ kJ mol^{-1}; $\Delta H^{0'} = -565.9$ kJ mol^{-1}

Forming ethanol from $5H_2$, CO and CO_2 (reaction (1) + (2)) is exothermic by −344.6 kJ mol^{-1} to be compared with the enthalpy change of −1,711.2 kJ mol^{-1} associated with the combustion of $5H_2$ and 1CO (2.5 × reaction (7) + 0.5 × reaction (8)). Thus, when forming ethanol from syngas only (344.6/ 1,711.2) × 100 = 20.14% of the enthalpy change associated with the combustion of H_2 and CO is liberated as heat. Therefore, the efficiency of energy conversion in syngas fermentation to ethanol (reaction (1) + (2)) is almost 80%.

The energy conversion efficiency of the formation of butanol (reaction (9)) and hexanol (reaction (10)) from CO, H_2 and CO_2 was calculated from the enthalpy changes associated with reactions (7)–(10) to be near 78%. Reaction (9) = reactions (1), (2), (3) and (5); and reaction (10) = reactions (1), (2), (3), (4) and (6).

$$10H_2 + 2CO + 2CO_2 \rightarrow CH_3CH_2CH_2CH_2OH + 5H_2O \quad (9)$$

$\Delta G^{0'} = -283.9$ kJ mol^{-1}; $\Delta H^{0'} = -747.4$ kJ mol^{-1}

$$15H_2 + 3CO + 3CO_2 \rightarrow CH_3CH_2CH_2CH_2CH_2CH_2OH + 8H_2O \quad (10)$$

$\Delta G^{0'} = -453.4$ kJ mol^{-1}; $\Delta H^{0'} = -1152.4$ kJ mol^{-1}

Calculation of the alcohol yield per kWh. The amount of butanol and hexanol obtained per kWh by electroreduction of CO_2 was calculated as follows: butanol contains 24 mol electrons and hexanol 36 mol electrons per mol. Assuming butanol and hexanol are being formed at a molar ratio of 1:1 then per mol of the two alcohols 30 mol electrons are required from electricity. One mol of electrons equals 96,485.3 coulomb. One coulomb per second = 1 A. Per mol alcohols CO and H_2 are required in a molar ratio of 1:5. When the CO_2 electrolyser is run at 4.7 V (Fig. 2c) and the H_2O electrolyser at 2.0 V, then on average both together run at 2.45 V. One V·A = 1 W = 2.45 V·0.41 coulomb s^{-1}. In 1 h at 1 kW 0.41 coulomb add up to 1,475,000 coulomb = 15.29 mol electrons equivalent to 0.51 mol butanol/hexanol = 44.88 g butanol/hexanol.

Calculation of costs per kWh. The costs of butanol and hexanol obtained per kWh by electro-reduction of CO_2 was calculated from a price of 1 kWh = 2.5 cents (http://cleantechies.com/2016/09/20/jinkosolar-marubeni-score-lowest-ever-solar-pv-at-us%C2%A22-42kwh-in-abu-dhabi)[57] and from that of butanol = 1.2€ per kg (ref. [1]). The costs of CO_2 separation and purification are presently around 60€ per t = 0.276 cents per mol CO_2 (ref. [58]) but is expected to decrease significantly through improved separation and purification systems and carbon trading in the near future[59]. For the synthesis of butanol and hexanol in a molar ratio of 1:1, 5 mol of CO_2 is required.

Data availability. All data are available from the corresponding author upon reasonable request.

Received: 5 May 2017; Accepted: 23 October 2017;
Published online: 8 January 2018

References

1. Malveda, M. P., Liu, S., Passararat, S. & Sesto, B. *Chemical Economics Handbook: Plasticizer Alcohols (C_4–C_{13})* 8,86 (IHS Chemical, 2015).
2. Kim, D., Sakimoto, K. K., Hong, D. C. & Yang, P. D. Artificial photosynthesis for sustainable fuel and chemical production. *Angew. Chem. Int. Ed.* **54**, 3259–3266 (2015).
3. Ganesh, I. Solar fuels vis-a-vis electricity generation from sunlight: the current state-of-the-art (a review). *Renew. Sust. Energ. Rev.* **44**, 904–932 (2015).
4. Karkas, M. D., Verho, O., Johnston, E. V. & Akermark, B. Artificial photosynthesis: molecular systems for catalytic water oxidation. *Chem. Rev.* **114**, 11863–12001 (2014).
5. Scott, E. L., Bruins, M. E. & Sanders, J. P. M. *Rules for the Bio-Based Production of Bulk Chemicals on a Small Scale: Can the Production of Bulk Chemicals on Small Scale be Competitive?* 1–36 (Agrotechnology and Food Science Group, Wageningen UR/Biobased Commodity Chemistry, 2013).
6. Clomburg, J. M., Crumbley, A. M. & Gonzalez, R. Industrial biomanufacturing: the future of chemical production. *Science* **355**, aag0804 (2017).
7. Woo, H. M. Solar-to-chemical and solar-to-fuel production from CO_2 by metabolically engineered microorganisms. *Curr. Opin. Biotechnol.* **45**, 1–7 (2017).
8. Jiao, F. et al. Selective conversion of syngas to light olefins. *Science* **351**, 1065–1068 (2016).
9. Polman, A., Knight, M., Garnett, E. C., Ehrler, B. & Sinke, W. C. Photovoltaic materials: present efficiencies and future challenges. *Science* **352**, aad4424 (2016).
10. Liew, F. et al. Metabolic engineering of *Clostridium autoethanogenum* for selective alcohol production. *Metabol. Eng.* **40**, 104–114 (2017).
11. Mock, J. et al. Energy conservation associated with ethanol formation from H_2 and CO_2 in *Clostridium autoethanogenum* involving electron bifurcation. *J. Bacteriol.* **197**, 2965–2980 (2015).
12. Dürre, P. Butanol formation from gaseous substrates. *FEMS Microbiol. Lett.* **363**, fnw040 (2016).
13. von der Assen, N., Muller, L. J., Steingrube, A., Voll, P. & Bardow, A. Selecting CO_2 sources for CO_2 utilization by environmental-merit-order curves. *Environ. Sci. Technol.* **50**, 1093–1101 (2016).
14. Hori, Y. & Suzuki, S. Electrolytic reduction of bicarbonate ion at a mercury-electrode. *J. Electrochem. Soc.* **130**, 2387–2390 (1983).
15. Asadi, M. et al. Nanostructured transition metal dichalcogenide electrocatalysts for CO_2 reduction in ionic liquid. *Science* **353**, 467–470 (2016).
16. Gao, S. et al. Partially oxidized atomic cobalt layers for carbon dioxide electroreduction to liquid fuel. *Nature* **529**, 68–71 (2016).
17. Neubauer, S. S., Krause, R. K., Schmid, B., Guldi, D. M. & Schmid, G. Overpotentials and Faraday efficiencies in CO_2 electrocatalysis-the impact of 1-ethyl-3-methylimidazolium trifluoromethanesulfonate. *Adv. Energy Mater.* **6**, 1502231 (2016).
18. Verma, S., Lu, X., Ma, S. C., Masel, R. I. & Kenis, P. J. A. The effect of electrolyte composition on the electroreduction of CO_2 to CO on Ag-based gas diffusion electrodes. *Phys. Chem. Chem. Phys.* **18**, 7075–7084 (2016).
19. Aoi, S., Mase, K., Ohkubo, K. & Fukuzumi, S. Selective electrochemical reduction of CO_2 to CO with a cobalt chlorin complex adsorbed on multi-walled carbon nanotubes in water. *Chem. Commun.* **51**, 10226–10228 (2015).
20. Kang, P., Chen, Z. F., Brookhart, M. & Meyer, T. J. Electrocatalytic reduction of carbon dioxide: let the molecules do the work. *Top. Catal.* **58**, 30–45 (2015).
21. Dufek, E. J., Lister, T. E., Stone, S. G. & McIlwain, M. E. Operation of a pressurized system for continuous reduction of CO_2. *J. Electrochem. Soc.* **159**, F514–F517 (2012).

22. Schreier, M. et al. Efficient photosynthesis of carbon monoxide from CO_2 using perovskite photovoltaics. *Nat. Commun.* **6**, 7326 (2015).
23. Schreier, M. et al. Solar conversion of CO_2 to CO using Earth-abundant electrocatalysts prepared by atomic layer modification of CuO. *Nat. Energy* **2**, 17087 (2017).
24. Turek, T., Moussallem, I., Bulan, A., Schmitz, N. & Weuta, P. Oxygen-consuming electrode with multilayer catalytic coating and process for the production thereof. US patent 9,243,337 B2 (2016).
25. Seitz, L. C. et al. A highly active and stable IrOx/$SrIrO_3$ catalyst for the oxygen evolution reaction. *Science* **353**, 1011–1014 (2016).
26. Seh, Z. W. et al. Combining theory and experiment in electrocatalysis: Insights into materials design. *Science* **355**, eaad4998 (2017).
27. Hatsukade, T., Kuhl, K. P., Cave, E. R., Abram, D. N. & Jaramillo, T. F. Insights into the electrocatalytic reduction of CO_2 on metallic silver surfaces. *Phys. Chem. Chem. Phys.* **16**, 13814–13819 (2014).
28. Mazloomi, K., Sulaiman, N. B. & Moayedi, H. Electrical efficiency of electrolytic hydrogen production. *Int. J. Electrochem. Sci.* **7**, 3314–3326 (2012).
29. Liew, F. et al. Gas fermentation: a flexible platform for commercial scale production of low-carbon-fuels and chemicals from waste and renewable feedstocks. *Front. Microbiol.* **7**, 27242719 (2016).
30. Angenent, L. T. et al. Chain elongation with reactor microbiomes: open-culture biotechnology to produce biochemicals. *Environ. Sci. Technol.* **50**, 2796–2810 (2016).
31. Bertsch, J. & Müller, V. Bioenergetic constraints for conversion of syngas to biofuels in acetogenic bacteria. *Biotechnol. Biofuels* **8**, 26692897 (2015).
32. Wang, S. N. et al. NADP-specific electron-bifurcating [FeFe]-hydrogenase in a functional complex with formate dehydrogenase in *Clostridium autoethanogenum* grown on CO. *J. Bacteriol.* **195**, 4373–4386 (2013).
33. Jones, S. W. et al. CO_2 fixation by anaerobic non-photosynthetic mixotrophy for improved carbon conversion. *Nat. Commun.* **7**, 12800 (2016).
34. Torella, J. P. et al. Efficient solar-to-fuels production from a hybrid microbial-water-splitting catalyst system. *Proc. Natl Acad. Sci. USA* **112**, 2337–2342 (2015).
35. Liu, C., Colon, B. C., Ziesack, M., Silver, P. A. & Nocera, D. G. Water splitting-biosynthetic system with CO_2 reduction efficiencies exceeding photosynthesis. *Science* **352**, 1210–1213 (2016).
36. Li, H. et al. Integrated electromicrobial conversion of CO_2 to higher alcohols. *Science* **335**, 1596–1596 (2012).
37. Seedorf, H. et al. The genome of *Clostridium kluyveri*, a strict anaerobe with unique metabolic features. *Proc. Natl Acad. Sci. USA* **105**, 2128–2133 (2008).
38. Li, F. et al. Coupled ferredoxin and crotonyl coenzyme a (CoA) reduction with NADH catalyzed by the butyryl-CoA dehydrogenase/Etf complex from *Clostridium kluyveri*. *J. Bacteriol.* **190**, 843–850 (2008).
39. Perez, J. M., Richter, H., Loftus, S. E. & Angenent, L. T. Biocatalytic reduction of short-chain carboxylic acids into their corresponding alcohols with syngas fermentation. *Biotechnol. Bioeng.* **110**, 1066–1077 (2013).
40. Phillips, J. R. et al. Butanol and hexanol production in *Clostridium carboxidivorans* syngas fermentation: medium development and culture techniques. *Bioresource Technol.* **190**, 114–121 (2015).
41. Isom, C. E., Nanny, M. A. & Tanner, R. S. Improved conversion efficiencies for *n*-fatty acid reduction to primary alcohols by the solventogenic acetogen "Clostridium ragsdalei". *J. Ind. Microbiol. Biotechnol.* **42**, 29–38 (2015).
42. Napora-Wijata, K., Strohmeier, G. A. & Winkler, M. Biocatalytic reduction of carboxylic acids. *Biotechnol. J.* **9**, 822–843 (2014).
43. Choi, J. I. & Lee, S. Y. Process analysis and economic evaluation for poly(3-hydroxybutyrate) production by fermentation. *Bioprocess. Eng.* **17**, 335–342 (1997).
44. Hermann, T. Industrial production of amino acids by coryneform bacteria. *J. Biotechnol.* **104**, 155–172 (2003).
45. Bohlmann, G. M. & Bray, R. *Biobutanol* Report No. 264 (SRI Consulting, Menlo Park, CA, 2008).
46. Bohlmann, G. M. & Cesar, M. A. *Ethanol Production in Brazil* Report No. 149A (SRI Consulting, Menlo Park, CA, 2006).
47. Bell, S. *Bio-Based Succinic Acid* (IHS, 2014).
48. Thauer, R. K., Jungerma., K., Henninge., H., Wenning, J. & Decker, K. Energy metabolism of *Clostridium kluyveri*. *Eur. J. Biochem* **4**, 173–180 (1968).
49. *Reports & Markets: Global and Chinese Natural Hexyl Alcohols* Report No. CAS 111-27-3 (360 Market Updates, Pune, 2016).
50. Camara Greiner, E. O., Blagoev, M. & Yamaguchi, Y. *Chemical Economics Handbook: Linear Alpha-Olefines* (IHS Chemical, 2013).
51. Schink, B., Kremer, D. R. & Hansen, T. A. Pathway of propionate formation from ethanol in *Pelobacter propionicus*. *Arch. Microbiol.* **147**, 321–327 (1987).
52. Hu, P. et al. Integrated bioprocess for conversion of gaseous substrates to liquids. *Proc. Natl Acad. Sci. USA* **113**, 3773–3778 (2016).
53. Li, X., Trevethick, S. & Cossey, B. J. Improved fermentation of gaseous substrates. Patent WO 2015/016722 A1 (2015).
54. Jörissen, J., Turek, T. & Weber, R. A silver-based oxygen depolarized cathode (ODC). *Chemie in unserer Zeit* **45**, 172–183 (2011).
55. Dufek, E. J., Lister, T. E. & McIlwain, M. E. Influence of S-contamination on CO_2 reduction at Ag electrodes. *J. Electrochem. Soc.* **158**, B1384–B1390 (2011).
56. Thauer, R. K., Jungermann, K. & Decker, K. Energy-conservation in chemotropic anaerobic bacteria. *Bacteriol. Rev.* **41**, 100–180 (1977).
57. Haegel, N. M. et al. Terawatt-scale photovoltaics: trajectories and challenges. *Science* **356**, 141–143 (2017).
58. Xu, G. et al. An improved CO_2 separation and purification system based on cryogenic separation and distillation theory. *Energies* **7**, 3484–3502 (2014).
59. Service, R. F. Cost of carbon capture drops, but does anyone want it? *Science* **354**, 1362–1363 (2016).
60. Diender, M., Stams, A. J. M. & Sousa, D. Z. Production of medium-chain fatty acids and higher alcohols by a synthetic co-culture grown on carbon monoxide or syngas. *Biotechnol. Biofuels* **9**, 27042211 (2016).

Acknowledgements

The authors thank R. K. Thauer (Max Planck Institute for Terrestrial Microbiology, Marburg) for his help in preparing the manuscript. Evonik Creavis GmbH (T.H. and M.D.), Siemens AG (R.K. and G.S.) and Covestro AG (R.W.) thank the German Federal Ministry of Education and Research (BMBF) for funding part of this work within the Kopernikus Initiative 'Power-to-X' under contract number P2X-03SFK2J0.

Author contributions

G.S. and R.W. discovered the potential of oxygen depolarized cathodes (ODC) for electrochemical CO_2-reduction. T.H. and M.D. are responsible for the fermentation part. G.S. and R.K. are responsible for the electrochemical part. M.D. and R.K. performed the laboratory work. G.S. and T.H. are heading the corresponding technology programmes at Siemens AG and Evonik Creavis GmbH, respectively, and wrote the paper.

Competing interests

The authors declare no competing financial interests.

Additional information

Supplementary information is available for this paper at https://doi.org/10.1038/s41929-017-0005-1.

Reprints and permissions information is available at www.nature.com/reprints.

Correspondence and requests for materials should be addressed to G.S.

Publisher's note: Springer Nature remains neutral with regard to jurisdictional claims in published maps and institutional affiliations.